

RESEARCH ARTICLE

Comparative analysis of gene expression identifies distinct molecular signatures of bone marrow- and periosteal-skeletal stem/progenitor cells

Lorenzo Deveza¹, Laura Ortinou², Kevin Lei², Dongsu Park^{2,3*}

1 Department of Orthopaedic Surgery, Baylor College of Medicine, Houston, TX, United States of America, **2** Department of Molecular and Human Genetics, Baylor College of Medicine, Houston, TX, United States of America, **3** Department of Immunology and Pathology, Baylor College of Medicine, Houston, TX, United States of America

* Dongsu.park@bcm.edu



OPEN ACCESS

Citation: Deveza L, Ortinou L, Lei K, Park D (2018) Comparative analysis of gene expression identifies distinct molecular signatures of bone marrow- and periosteal-skeletal stem/progenitor cells. *PLoS ONE* 13(1): e0190909. <https://doi.org/10.1371/journal.pone.0190909>

Editor: Jung-Eun Kim, Kyungpook National University School of Medicine, REPUBLIC OF KOREA

Received: November 2, 2017

Accepted: December 21, 2017

Published: January 17, 2018

Copyright: © 2018 Deveza et al. This is an open access article distributed under the terms of the [Creative Commons Attribution License](https://creativecommons.org/licenses/by/4.0/), which permits unrestricted use, distribution, and reproduction in any medium, provided the original author and source are credited.

Data Availability Statement: The microarray data is available from the GEO database under the accession number GSE107798.

Funding: Research reported in this publication was supported by National Institute of Arthritis and Musculoskeletal and Skin Diseases of the National Institutes of Health under grant number 1K01AR061434 and by the Bone Disease Program of Texas Award to D.P and The Caroline Wiess Law Fund Award to DP. The funders had no role in

Abstract

Periosteum and bone marrow (BM) both contain skeletal stem/progenitor cells (SSCs) that participate in fracture repair. However, the functional difference and selective regulatory mechanisms of SSCs in different locations are unknown due to the lack of specific markers. Here, we report a comprehensive gene expression analysis of bone marrow SSCs (BM-SSCs), periosteal SSCs (P-SSCs), and more differentiated osteoprogenitors by using reporter mice expressing Interferon-inducible *Mx1* and *Nestin*^{GFP}, previously known SSC markers. We first defined that the BM-SSCs can be enriched by the combination of *Mx1* and *Nestin*^{GFP} expression, while endogenous P-SSCs can be isolated by positive selection of *Mx1*, CD105 and CD140a (known SSC markers) combined with the negative selection of CD45, CD31, and *osteocalcin*^{GFP} (a mature osteoblast marker). Comparative gene expression analysis with FACS-sorted BM-SSCs, P-SSCs, *Osterix*⁺ preosteoblasts, CD51⁺ stroma cells and CD45⁺ hematopoietic cells as controls revealed that BM-SSCs and P-SSCs have high similarity with few potential differences without statistical significance. We also found that CD51⁺ cells are highly heterogeneous and have little overlap with SSCs. This was further supported by the microarray cluster analysis, where the two SSC populations clustered together but are separate from the CD51⁺ cells. However, when comparing SSC population to controls, we found several genes that are uniquely upregulated in endogenous SSCs. Amongst these genes, we found KDR (aka Flk1 or VEGFR2) to be most interesting and discovered that it is highly and selectively expressed in P-SSCs. This finding suggests that endogenous P-SSCs are functionally very similar to BM-SSCs with undetectable significant differences in gene expression but there are distinct molecular signatures in P-SSCs, which can be useful to specify P-SSC subset *in vivo*.

study design, data collection and analysis, decision to publish, or preparation of the manuscript.

Competing interests: The authors have declared that no competing interests exist.

Introduction

Bone fractures constitute a significant burden to the healthcare system with about 16 million fractures per year in the United States. Majority of fractures heal with adequate treatment, but about 5–10% go on to non-union [1]. Treatment methods include bone grafting, delivery of growth factors, and cell-based therapies. Fundamentally, these attempts to augment the healing process are attempts to stimulate the cells that drive fracture repair [2,3]. Studies on such therapeutic attempts are based on using or stimulating bone marrow skeletal stem cells (BM-SSCs), also known as bone marrow mesenchymal stem cells (BMSCs) [4]. However, endogenous SSCs are a heterogeneous population and are present in multiple tissue locations including periosteum [5]. It is known that SSCs are necessary for fracture repair, yet whether SSCs in different locations have the same functional properties or if they have distinct functions and regulation necessary for the repair process remain unknown.

At its core, bone fracture healing is a complex process that involves the interplay of multiple cell types derived from different tissue sources. Bone marrow (BM) and periosteum are two of the surrounding tissues intimately involved in fracture repair [6]. However, BM is not necessary for healing to proceed, while removal of periosteal tissues can cause non-union [7]. Indeed, this is a fundamental principle in clinical fracture management. This is further exemplified by cell-labeling studies demonstrating that the major cellular contributors to the fracture callus are periosteal cells [8,9]. More importantly, it has been reported that P-SSCs may have differing functions than BM-SSCs, whereby P-SSCs display endochondral ossification and intramembranous bone formation, while BM-SSCs only participate in the latter process [10,11]. These differences suggest that P-SSCs may have different inherent properties compared to BM-SSCs.

Although there is much progress in defining unique gene expression patterns in postnatal skeletal stem cells [12], to date, little is known about the potential differences between P-SSCs and BM-SSCs. This is partly because no reliable markers exist to isolate each of these cell populations to enable such study. Studies on mouse BM-SSCs have identified multiple markers that isolate a potentially more highly purified population of these cells, including *Nestin*^{GFP} [13], *LepR*^{Cre} (Leptin Receptor) [14], and *Grem1*^{Cre-ERT} (Gremlin 1) [15]. Previously, *Myxovirus resistance 1* (*Mx1*) was also shown to identify long-term resident skeletal stem/progenitor cells in mice via *in vivo* imaging experiments consistent with their role as BM-SSCs [16]. While fewer markers exist for P-SSCs, *Mx1*⁺ cells are also known to reside within the periosteal compartment [16], and these cells provide downstream osteolineage cells enabling their potential use for studying P-SSCs endogenously.

In this study, we isolated BM-SSCs and P-SSCs from transgenic mice based on expression of *Mx1* promoter. BM-SSCs were isolated from BM tissues in transgenic mice expressing *Mx1*^{Cre} and *Nestin*^{GFP} (*Mx1*⁺*Nes*^{GFP+} cells), known SSC markers. P-SSCs were isolated from periosteal tissues in *Mx1*^{Cre}; *Rosa*^{Tomato}; *Osteocalcin*^{GFP} reporter mice, whereby P-SSCs were negatively selected against *Osteocalcin*^{GFP+} osteoblasts (*Mx1*⁺*Ocn*⁻ cells). Microarray was run on each of these cell populations, using CD45⁺ cells and *Osterix*⁺ (*Osx*⁺) osteolineage cells as controls. We further compared CD140a⁺CD51⁺ cells as an additional BMSC population reported in literature [17]. Lastly, we identify a potentially novel marker for mouse P-SSCs.

Materials and methods

Mice

Four to six-week old C57BL/6, *Mx1*^{Cre} [18], *Rosa26-loxP-stop-loxP-tdTomato* (*Rosa*-Tom) [19] mice were purchased from The Jackson laboratory. *Osteocalcin*^{GFP} [20,21] and *Nestin*^{GFP} [22]

(C57/BL6 background) mice were kindly provided by Dr. Henry Kronenberg. Genotyping of all Cre-transgenic mice and the Rosa locus was performed by PCR (GenDEPOT) according to The Jackson laboratory's protocols. At 4-week age, all *Mx1* mice (*Mx1*^{Cre}; *Rosa*^{Tomato}; *Osteocalcin*^{GFP} or *Mx1*^{Cre}; *Rosa*^{Tomato}; *Nestin*^{GFP}) were lethally irradiated with 9.5 Gy and transplanted with 10⁶ whole bone marrow cells from wild-type C57BL/6 mice (WT-BMT). At six to eight weeks later (when host hematopoietic cells are less than 1%), *Mx1*^{Cre} activity was induced by intraperitoneal injection of 25 mg/kg of polyinosinic:polycytidylic acid (pIpC, Sigma) every other day for 10 days as described previously [13]. At the indicated time after pIpC induction, mice were subjected to *in vivo* imaging experiments. All mice were maintained in pathogen-free conditions, and all procedures were approved by Baylor College of Medicine's Institutional Animal Care and Use Committee (IACUC).

Intravital imaging

For *in vivo* imaging of fluorescent cells in living animals, mice were anesthetized with Combo-III and prepared for a customized two-photon and confocal hybrid microscope (Leica TCS SP8MP with DM6000CFS) specifically designed for live animal imaging, as described in our previous report [16,21]. Briefly, a small incision was introduced on the scalp of *Mx1*/Tomato/*Ocn*-GFP or *Mx1*/Tomato/*Nestin*-GFP mice and the surface of calvaria near the intersection of sagittal and coronal suture was exposed. The mice were then mounted on a 3-D axis motorized stage (Anaheim Automation Anaheim, CA), and the calvarial surface was scanned for second harmonic generation (SHG by femto-second titanium:sapphire laser pulses: 880 nm) from bones to identify the injury sites and the intersection of sagittal and coronal sutures. GFP-expressing cells (488 nm excitation, 505–550 nm detection) and Tomato-expressing cells (561 nm excitation, 590–620 nm detection) were simultaneously imaged by confocal spectral fluorescence detection. All images were recorded with their distances to the intersection of the sagittal and coronal sutures to define their precise location. After *in vivo* imaging, the scalp was closed using a VICRYL plus suture (Ethicon) as previously described [16]. 3-D Images were reconstructed using the Leica Application Suite software, and osteoblasts were counted.

Post-operative care and Euthanasia

Post-operative care was provided as previously described [16]. Mice were anesthetized with Rodent III (BCM CCM combination with anesthetic DEA-III). Each ml of Rodent III contains ketamine 37.5 mg, xylazine 1.9 mg and acepromazine 0.37 mg (5 ml with 2.45 ml sterile water) and was given at 0.75–1.5 ml/kg by intraperitoneal injection (~0.05 ml/30 g mouse). Mice were kept warm and monitored for recovery from anesthesia via toe pinch responses. For post manipulation, mice were monitored for any signs of infection or discomfort by following BCM-IACUC approved protocols. Animals were sacrificed by isoflurane anesthesia and by CO₂ at the termination of experiments or when discomfort was apparent. This method is consistent with the recommendations of the Panel of Euthanasia of the American Veterinary Medical Association and in BCM-IACUC approved protocols.

Isolation and flow cytometry analysis of mouse SSCs

To isolate periosteal cells, dissected femurs, tibias, pelvis and calvaria from mice were placed in PBS, and the overlying fascia, muscle, and tendon were carefully removed. The bones with periosteum were incubated in ice-cold PBS with 1% FBS for 30 min, and the loosely associated periosteum was peeled off using forceps, scalpel, and dissecting scissors. The soft floating periosteal tissues collected with a 40- μ m strainer were then incubated with 5–10 ml of 0.1% collagenase and 10% FBS in PBS at 37°C for 1 hour, and dissociated periosteal cells were washed

with PBS, filtered with a 40- μm strainer and resuspended at $\sim 1 \times 10^7$ cells/ml. To isolate cells from bones and bone marrow, dissected femurs, tibias and pelvis bones after periosteum removal were cracked with a pestle and rinsed 3 times to remove and collect bone marrow cells. The remaining bones were minced with a scalpel and/or a dissecting scissor and then incubated with 10 ml of 0.1% collagenase and 10% FBS in PBS at 37°C for 1 hour with strong vortexing every 10 minute. Dissociated cells were washed with PBS, filtered with a 40- μm strainer and resuspended at $\sim 1 \times 10^7$ cells/ml. To analyze or isolate SSCs and osteogenic cells, cells were stained with CD105-PE-Cy7 (clone: MJ7/18), CD140a-APC (clone: APA5), CD45-pacific blue (clone: 30-F11), Ter119-APC-Cy7 (clone: TER-119), and CD31-eFlour 450 (clone: 390) in combination with KDR-PE-Cy7 (clone: J073E5). Antibodies were purchased from eBioscience unless otherwise stated. Propidium iodide or DAPI was used for viable cell gating. Flow cytometric experiments and sorting were performed using the LSRII and FACS Aria cytometer (BD Biosciences, San Jose, CA). Data were analyzed with the FlowJo software (TreeStar, Ashland, OR) and represented as histograms, contour, or dot plots of fluorescence intensity.

Microarray analysis

Sorted cells from two or three male and female mice were used to isolate RNA using the RNeasy Micro kit (Qiagen), according to the manufacturer's instructions. Purified RNA was reverse-transcribed, amplified, and labeled with the Affymetrix Gene Chip whole transcript sense target labeling kit. Labeled cDNA (2 biological repeats) from indicated cells was analyzed using Affymetrix mouse A430 microarrays, according to the manufacturer's instructions, performed at the Dana-Farber Cancer Institute Microarray Core. CEL files (containing raw expression measurements) were imported to Partek GS, and data were preprocessed and normalized using the RMA (Robust Multichip Average) algorithm. The NIH GEO accession number for the microarray analysis data included in this paper is GSE107798.

Microarray data analysis and statistics

Microarray data was pre-processed for normalization and statistical differences using R statistical package. Normalization was done using a robust multichip average (RMA) technique. Statistical differences were calculated with the limma package in R. Post-processing cluster analysis was done using Cluster 3.0 software and were plotted using Java TreeView software. Scatter plots were generated using Orange biolab software. We assessed pairwise comparisons between each of the following groups: 1) $Mx1^+Ocn^-$ P-SSCs; 2) $Mx1^+Nes^+$ BM-SSCs; 3) CD45⁺ hematopoietic lineage cells; 4) $Osterix^{GFP+}$ osteoprogenitor cells [23]; and, 5) CD51⁺ BMSCs [24]. We evaluated the number of statistically different genes by changing the p-value statistical criteria for acceptance. We found that acceptance criteria of $p < 0.05$ provided at least 50 statistically different genes between controls and $Mx1^+$ SSCs.

Results

In vivo identification of BM-SSCs and P-SSCs

BM-SSCs and P-SSCs were derived from transgenic mice based on expression of interferon-induced GTP-Binding Protein *Mx1* promoter, which has been previously shown to represent long-term resident osteoprogenitor cells [16]. Here, $Mx1^{Cre}; Rosa^{Tomato}; Osteocalcin^{GFP}$ mice were used as previously described [21]. Using this model, we confirmed through pulse-chase labeling studies in native bone marrow tissue (i.e. no injury) that pulse-labeled $Mx1^+$ cells at day 5 are mainly $Osteocalcin^{GFP}$ negative (Ocn^-) and these $Mx1^+$ cells contribute to the

majority of new Ocn^+ osteoblasts at day 60 (yellow), demonstrating that $Mx1^+$ cells include skeletal stem/progenitor cells (SSCs), albeit far upstream of mature osteoblasts (Fig 1A). Considering that Ocn^+ cells represent mature osteolineage cells, we found that $Mx1^+Ocn^-$ upstream progenitors are present throughout bone marrow, as well as calvarial suture and periosteum (Fig 1B). We thus isolated P-SSCs from periosteal tissue by focusing on $Mx1^+Ocn^-$ cells within this tissue compartment. Specifically, we isolated P-SSCs by isolating cells from periosteum, negatively selecting for hematopoietic lineage cells ($CD45^-$), endothelial lineage cells ($CD31^-$), erythroid lineage ($Ter119^-$), and mature osteolineage cells (Ocn^-), and positively selecting for SSC markers including $Mx1^+$, $CD105^+$ and $CD140a^+$ (PDGFRa). We refer to these cells as $Mx1^+Ocn^-$ P-SSCs (Fig 1C).

BM-SSCs were isolated from $Mx1^{Cre}; Rosa26^{Tomato}; Nestin^{GFP}$ transgenic mice. $Nestin^{GFP}$ (Nes^+) is a well-studied marker for BM-SSCs [25]. By pulse-chase labeling studies, we found that $Mx1^+Nes^+$ cells are native perivascular cells that are present throughout BM and calvarial suture (Fig 1D), which is consistent with prior studies as BM-SSCs are generally known to be perivascular cells [13,26]. For our experiments, we isolated BM-SSCs using this model from the BM tissue compartment, which were sorted by negative selection of $CD45^-$, $CD31^-$, $Ter119^-$, as well as positive selection of $CD105^+$ and $CD140a^+$; finally, $Mx1^+Nes^+$ cells were selected from the remaining cells (Fig 1E). We referred to this subpopulation as $Mx1^+Nes^+$ BM-SSCs. Interestingly, we noted that the selection of BM-SSCs based on $CD45^-CD31^-Ter119^-CD105^+CD140a^+$ cells yields a heterogeneous mixture of $Mx1^+$ and $Nestin^+$ cells (Fig 1E).

Common selection criteria for BM-SSCs yields a heterogeneous mixture

To assess the functional genetic differences of BM-SSCs and P-SSCs, we performed microarray analysis of $Mx1^+Ocn^-$ P-SSCs and $Mx1^+Nes^+$ BM-SSCs. We added an additional BMSC population that was selected from the BM compartment based on $CD45^-CD31^-Ter119^-CD105^+CD140a^+$ selection, in addition to $CD51^+$, which is a commonly used selection criteria for BMSCs [17]. We refer to these cells as $CD51^+$ BMSCs. $CD45^+$ hematopoietic lineage cells and $Osterix^{GFP+}$ (Osx^+) osteoprogenitor cells were used as control populations [23,27]. From scatter plot analysis of all microarrayed genes, we found that each SSC population is a distinct population as compared to $CD45^+$ cells (Fig 2A–2C). We further defined that each SSC population are more closely related to Osx^+ osteolineage cells, but with multiple differentially expressed genes (Fig 2D–2F). Taken together, these scatter plots illustrated that each SSC population is similarly distinct from $CD45^+$ and Osx^+ cells.

Interestingly, we found that commonly used selection criteria for BMSCs may yield a heterogeneous mixture of cells, which is demonstrated by direct comparison between $Mx1^+Nes^+$ BM-SSCs and $CD51^+$ BMSCs (Fig 2G). Between these two cell populations there are 97 differentially expressed genes at $p < 0.01$ and 430 differentially expressed genes at $p < 0.05$. When comparing $Mx1^+Nes^+$ BM-SSCs with Nes^+ BMSCs (i.e. $Mx1^{-/-}$) there are no differentially expressed genes (Fig 2H). These findings suggest that considering both Nes^+ and $CD140a^+CD51^+$ have both been shown to represent BMSCs, that previously studied BMSCs are a heterogeneous mixture of cells.

P-SSCs and BM-SSCs are a similar population of cells

When directly comparing BM-SSCs with P-SSCs, we revealed that these cell populations are a similar population of cells. In our analysis, we found that $CD51^+$ BMSCs have several differentially expressed genes compared to $Mx1^+Ocn^-$ P-SSCs (Fig 2I), but there are few differences when comparing $Mx1^+Nes^+$ BM-SSCs with $Mx1^+Ocn^-$ P-SSCs and none is significant at the $p < 0.05$ acceptance criteria (Fig 2J). This is further summarized in the cluster plot, which

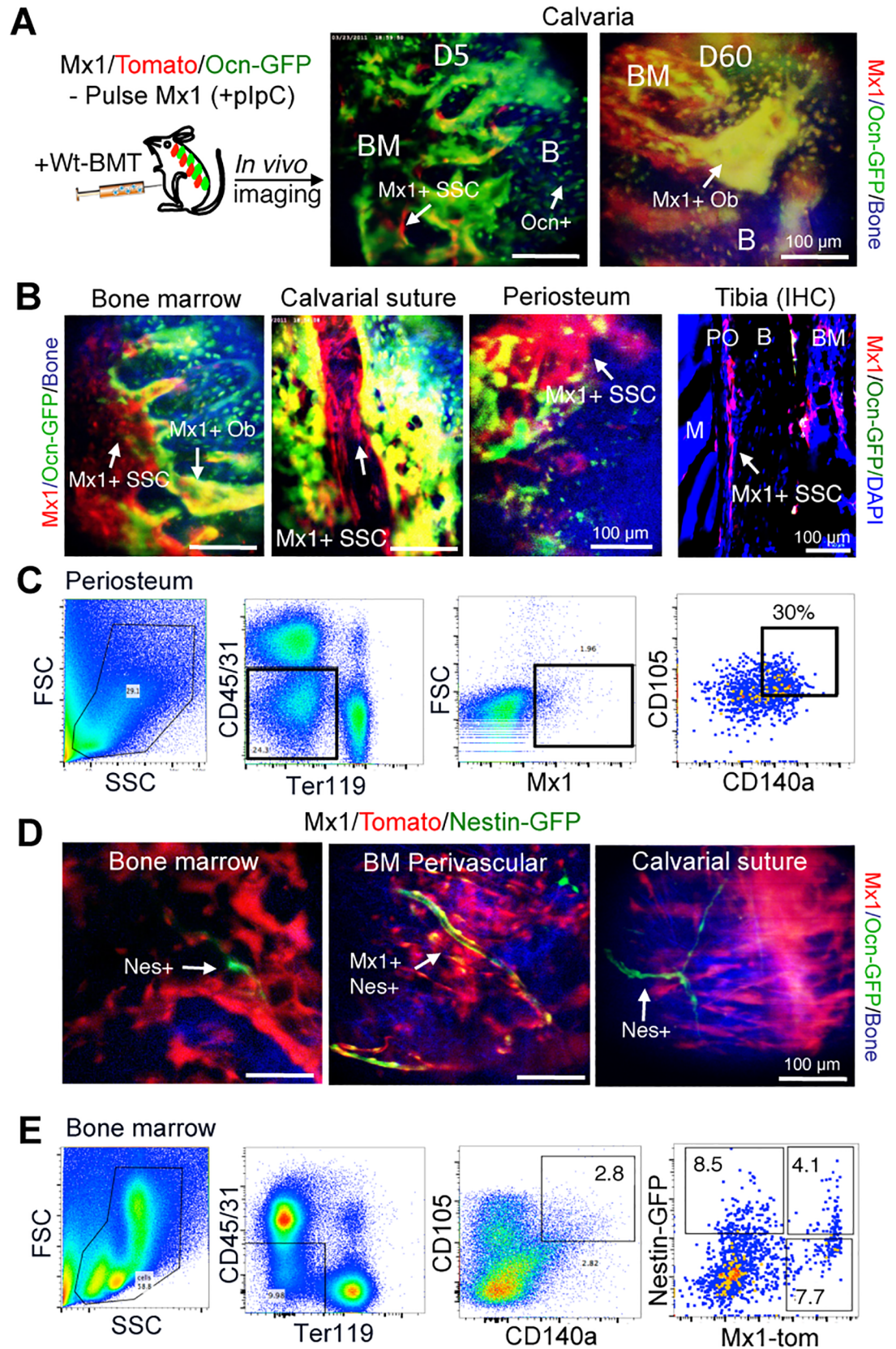


Fig 1. Functional identification of P-SSCs and BM-SSCs. (A) Interferon inducible $Mx1^+$ SSCs (red) are shown to contribute to majority osteoblasts (green, overlap yellow) *in vivo*. (B) $Mx1^+$ SSCs represent long-term osteolineage progenitor cells in BM and periosteal tissues. *In vivo* imaging shows that $Mx1^+$ SSCs reside in bone marrow, suture, and periosteum of calvarial bones. Immunofluorescent staining of tibial metaphysis of $Mx1$ /Tomato/Ocn-GFP mice shows that $Mx1^+$ SSCs (red, arrows) are abundant in periosteum (PO) (Tibia IHC). (C) P-SSCs from periosteal tissues are FACS-sorted by $CD45^-CD31^-Ter119^-CD105^+CD140a^+$ and $Mx1^+Ocn^-$, which are referred to as $Mx1^+Ocn^-$ P-SSCs. (D) $Mx1^+Nestin^+$ BM-SSCs are perivascular cells in BM but are undetectable in periosteum and calvarial suture. (E) $Mx1^+Nes^+$ cells within $CD45^-CD31^-Ter119^-CD105^+CD140a^+$ SSC fraction in bone marrow are isolated by FACS-sorting and are referred to as $Mx1^+Nes^+$ BM-SSCs. Notably, $CD105^+CD140a^+$ progenitors are heterogeneous $Mx1^+$ and $Nestin^+$ cells.

<https://doi.org/10.1371/journal.pone.0190909.g001>

demonstrated that $Mx1^+Nes^+$ BM-SSCs and $Mx1^+Ocn^-$ P-SSCs cluster together and are separate from $CD51^+$ BMSCs ($p < 0.05$, Fig 2K).

Determination of differentially expressed genes between P-SSCs and BM-SSCs with controls

Considering that there were no differentially expressed genes found between $Mx1^+Ocn^-$ P-SSCs and $Mx1^+Nes^+$ BM-SSCs, we proceeded to identify the genes that were differentially expressed between each of these populations and controls ($CD45^+$ and Osx^+ cells) separately. Cluster analysis of differentially expressed genes between $Mx1^+Ocn^-$ and controls is shown in Fig 3A and between $Mx1^+Nes^+$ BM-SSCs and controls is shown in Fig 3B. There were 101 differentially expressed genes between $Mx1^+Ocn^-$ P-SSCs compared to controls and 84 for $Mx1^+Nes^+$ BM-SSCs; while there were 55 overlapping differentially expressed genes for both SSC populations compared to controls (Fig 3C). Genes that were overexpressed are shown in S1 Table. Among the full list of differentially expressed genes, we identified several genes that are highly expressed in both SSC populations (Fig 3D). Interestingly, we found selectively increased expression of the vascular endothelial growth factor receptors (VEGFR), Flt1 (VEGFR1) and KDR (VEGFR2), in the P-SSC population compared to controls. In addition, we found that the level of KDR expression in P-SSCs is much higher than that of BM-SSCs although it is expressed in both SSC populations (Fig 3D), implicating that KDR can be a selective marker for P-SSCs.

P-SSCs are $CD140a^+KDR^+$ osteolineage progenitor cells

From our microarray analysis, we sought to further explore KDR expression in $Mx1^+Ocn^-$ P-SSCs and $Mx1^+Nes^+$ BM-SSCs. Notably, $CD140a^+KDR^+$ cells have been found to represent early mesoderm subpopulations [28]. We first compared our SSC populations to other publicly available SSC populations using Gene Expression Commons data (Fig 4A) [29]. We noted that other well-studied BM-SSC markers, Leptin receptor (LepR) and Gremlin 1 (Grem1) [30], were highly expressed in $Mx1^+Ocn^-$ P-SSCs and $Mx1^+Nes^+$ BM-SSCs, which demonstrated the consistency of our data with other known SSC populations (Fig 4A). By this same analysis, we found that KDR transcripts appeared to be much higher in $Mx1^+Ocn^-$ P-SSCs than $Mx1^+Nes^+$ BM-SSCs (Fig 4A). We confirmed these findings by RT-PCR (Fig 4B), which supported our microarray analysis.

We next assessed if KDR is a prospective surface marker for endogenous P-SSCs. We included P-SSCs ($CD45^-CD31^-Ter119^-CD105^+CD140a^+Mx1^+Ocn^-$), periosteal mature osteoblasts ($CD45^-CD31^-Ter119^-Mx1^+Ocn^+$), Nes^+ BMSCs ($CD45^-CD31^-Ter119^-CD140a^+Nes^+$), and $CD45^+$ cells from $Mx1^{Cre}; Rosa^{Tomato}$; *Osteocalcin*^{GFP} and $Mx1^{Cre}; Rosa^{Tomato}; Nestin^{GFP}$ mice. FACS analysis of these populations revealed that 77% of $Mx1^+Ocn^-$ P-SSCs express $CD140a$ and KDR, while only ~ 1% Ocn^+ mature osteoblasts (Fig 5A, $Ocn-GFP^+$), ~ 0.5% of $Mx1^+$ progenitors in the bone marrow (Fig 5B), and ~ 2% of Nes^+ BMSCs (Fig 5C)

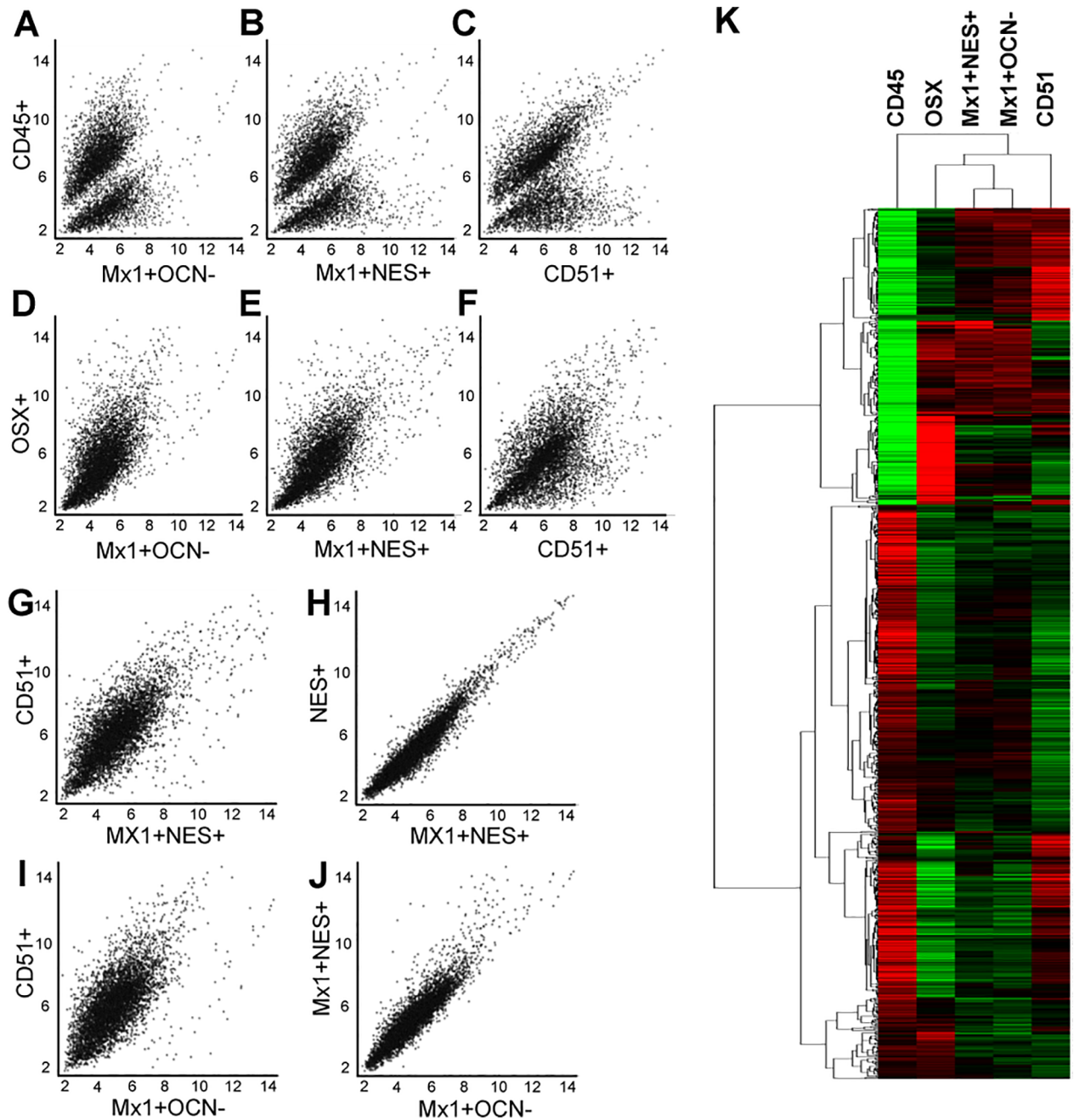


Fig 2. Commonly used markers for BM-SSCs yield a heterogeneous mixture, but are similar to P-SSCs. (A-C) Scatter plot comparison between *Mx1⁺Ocn⁻* P-SSCs (A), *Mx1⁺Nes⁺* BM-SSCs (B), and *CD51⁺* BMSCs (C) with *CD45⁺* cells, demonstrates that these populations are likewise different from *CD45⁺* hematopoietic cells from the BM compartment. (D-F) Scatter plot comparison between *Mx1⁺Ocn⁻* P-SSCs (D), *Mx1⁺Nes⁺* BM-SSCs (E), and *CD51⁺* BMSCs (F) with *Osx⁺* osteoprogenitor cells shows that each of these populations are more functionally similar to the osteolineage cells. (G) Direct comparison between *CD51⁺* BMSCs and *Mx1⁺Nes⁺* BM-SSCs demonstrates that these two commonly used selection markers for BM-SSCs yield a heterogeneous mixture of cells. (H) *Mx1⁺Nes⁺* BM-SSCs and *Nes⁺* cells are essentially the same population of cells. (I & J) Comparing *Mx1⁺Ocn⁻* P-SSCs with *CD51⁺* BMSCs (I) shows that these are functionally different cell-populations, but comparison with *Mx1⁺Nes⁺* BM-SSCs (J) shows few differences. (K) Cluster analysis of these cell populations confirms scatter plot analysis and shows that *Mx1⁺Ocn⁻* P-SSCs and *Mx1⁺Nes⁺* BM-SSCs cluster together, but each of these populations are distinct from *CD51⁺* BMSCs ($p < 0.05$).

<https://doi.org/10.1371/journal.pone.0190909.g002>

express these markers, implicating that P-SSCs specifically express KDR ($n = 3$, $p < 0.0001$, Fig 5D). To further confirm the KDR and CD140a expression in P-SSCs and to exclude a possible

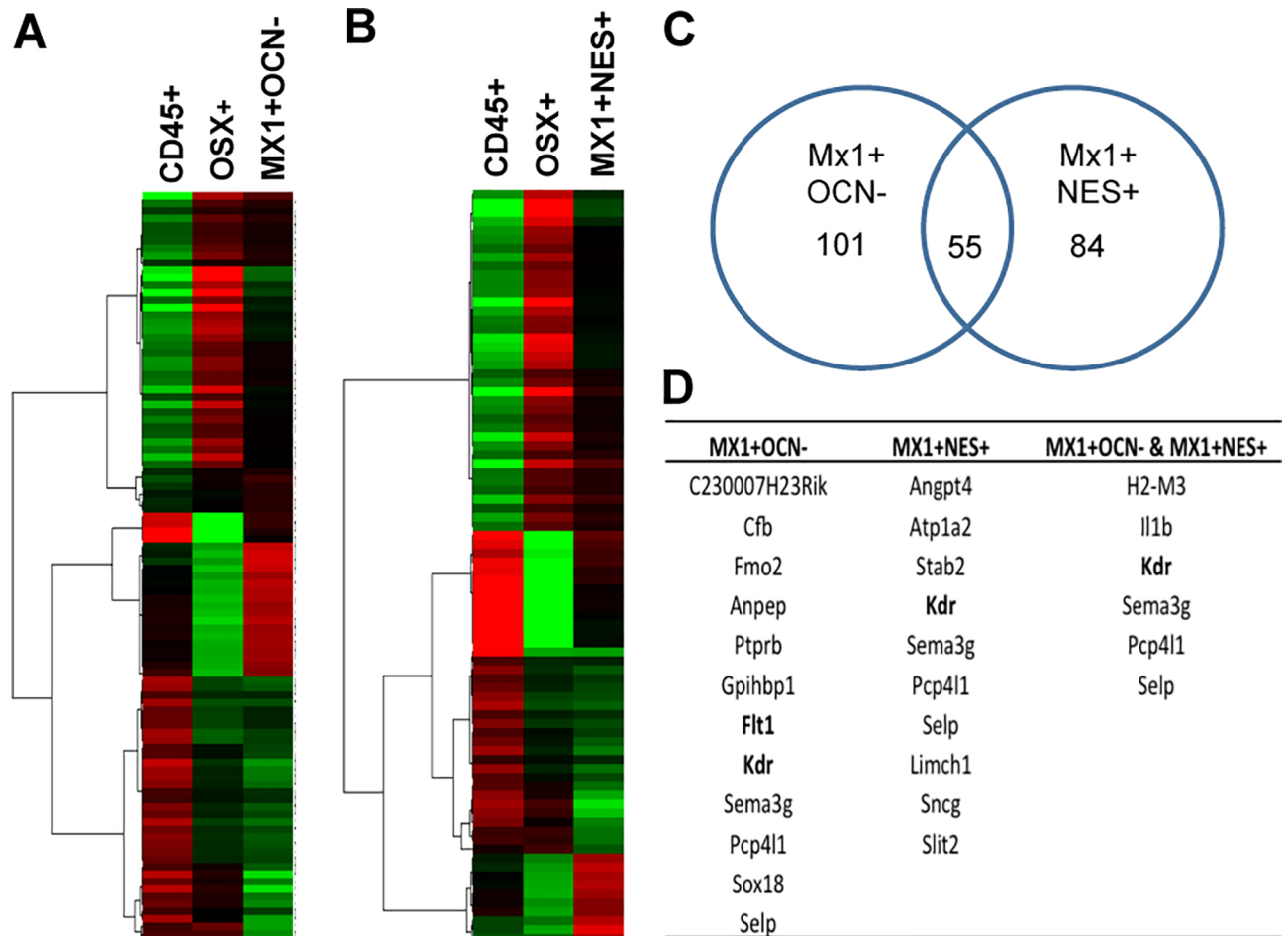


Fig 3. Identification of differentially expressed genes between P-SSCs and BM-SSCs and controls. (A & B) Differential gene expression between CD45⁺ cells and Osx⁺ cells with *Mx1*⁺*Ocn*⁻ P-SSCs (A) and *Mx1*⁺*Nes*⁺ BM-SSCs (B). (C) Number of differentially expressed genes between SSC populations and controls shows 101 for *Mx1*⁺*Ocn*⁻ P-SSCs, 84 for *Mx1*⁺*Nes*⁺ BM-SSCs, and 55 overlapping genes. (D) List of genes that were upregulated in SSCs compared to controls includes Flt1 (VEGF receptor 1) and KDR (VEGF receptor 2), despite removal of CD31 endothelial lineage cells from these populations.

<https://doi.org/10.1371/journal.pone.0190909.g003>

contamination of *Mx1*⁺*KDR*⁺ hematopoietic cells and endothelial cells, we employed *Prx1*^{GFP} mice, in which GFP expression is restricted in periosteal progenitor cells without detectable expression in hematopoietic and endothelial cells [31,32]. We found that ~ 76% of *Prx1*⁺ P-SSCs (CD45⁻CD31⁻Ter119⁻CD140a⁺ *Prx1*^{GFP+}) express KDR (Fig 5E, *Prx1*-GFP+), while *Prx1*⁻ cells have undetectable expression of KDR (Fig 5E, *Prx1*-GFP-). Thus, our microarray analysis reliably demonstrated differential gene expression in both BM-SSCs and P-SSCs and we found that P-SSCs have selectively high expression of KDR *in vivo*.

Discussion

Herein, we sought to assess the functional genetic differences between mouse BM-SSCs and P-SSCs. These cell populations display differing apparent roles in fracture repair, so we hypothesized that their differences would be borne out in genetic expression analyses. We used *Mx1*⁺*Nes*^{GFP+} cells from BM as BM-SSCs and *Mx1*⁺*Ocn*^{GFP-} cells from periosteal tissues as P-SSCs. With these cells, we performed a microarray analysis to compare their functional genetic differences. However, we were unable to find statistically significant difference in gene

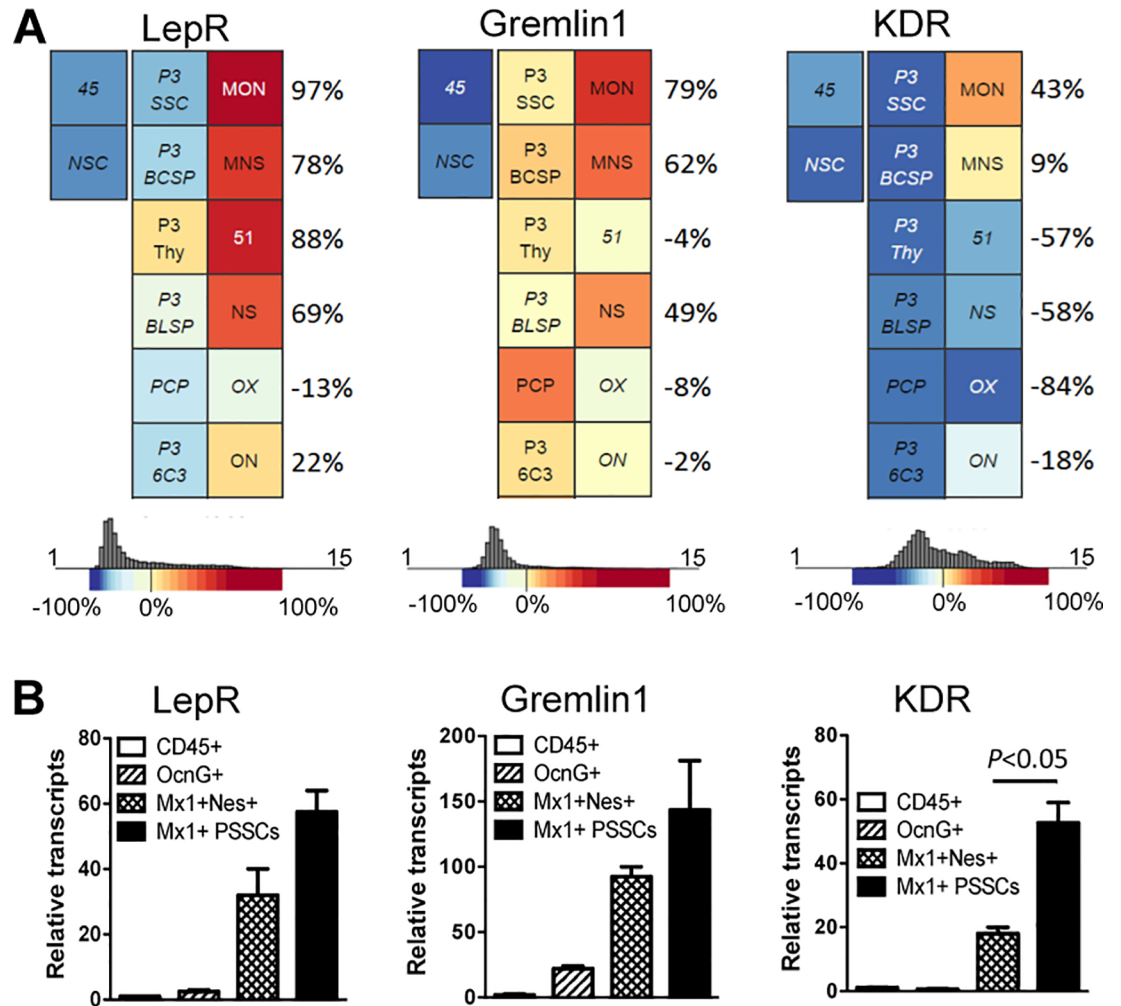


Fig 4. P-SSCs and BM-SSCs express common SSC markers. (A) Gene commons analysis shows that $Mx1^{+}Ocn^{-}$ P-SSCs (MON) and $Mx1^{+}Nes^{+}$ BM-SSCs (MNS) highly express Leptin receptor (LepR) and Gremlin 1, demonstrating that these SSC populations share characteristics with previously studied early postnatal SSC and progenitor populations [29]. Further, KDR is found to be uniquely expressed in P-SSCs compared to other SSCs. (B) Hematopoietic cells (CD45⁺), osteoblasts (OcnG⁺), $Mx1^{+}Nes^{+}$ BM-SSCs (MNS) and $Mx1^{+}$ P-SSCs were sorted, and the levels of the indicated genes were quantified by qPCR.

<https://doi.org/10.1371/journal.pone.0190909.g004>

expression of these two populations. This is not unexpected considering that these both represent skeletal stem/progenitor cell populations, albeit from differing sources. On further analysis, we did find a novel marker for P-SSCs in comparison to BM-SSCs, which was KDR (aka VEGFR2, Fig 5D & 5E). Additionally, there were other potential candidate genes upregulated in each SSC population in comparison to controls but their functional significance was unclear. Thus, while we did not find differential gene expression by clustered microarray analysis, we were able to find few unique genetic differences suggesting that these two cell populations may have subtle but critical functional differences.

Among the several markers previously demonstrated for SSCs, including Gremlin 1 [30], Leptin Receptor and Nestin [25], we chose to isolate SSCs based on expression of $Mx1$. Unlike other markers, $Mx1^{+}$ cells were shown to contribute to adult osteolineage cells by live *in vivo* imaging. This was further demonstrated here, which confirms their identity as osteolineage cells (Fig 1A). Given $Mx1$ marker has been known to label upstream hematopoietic lineage

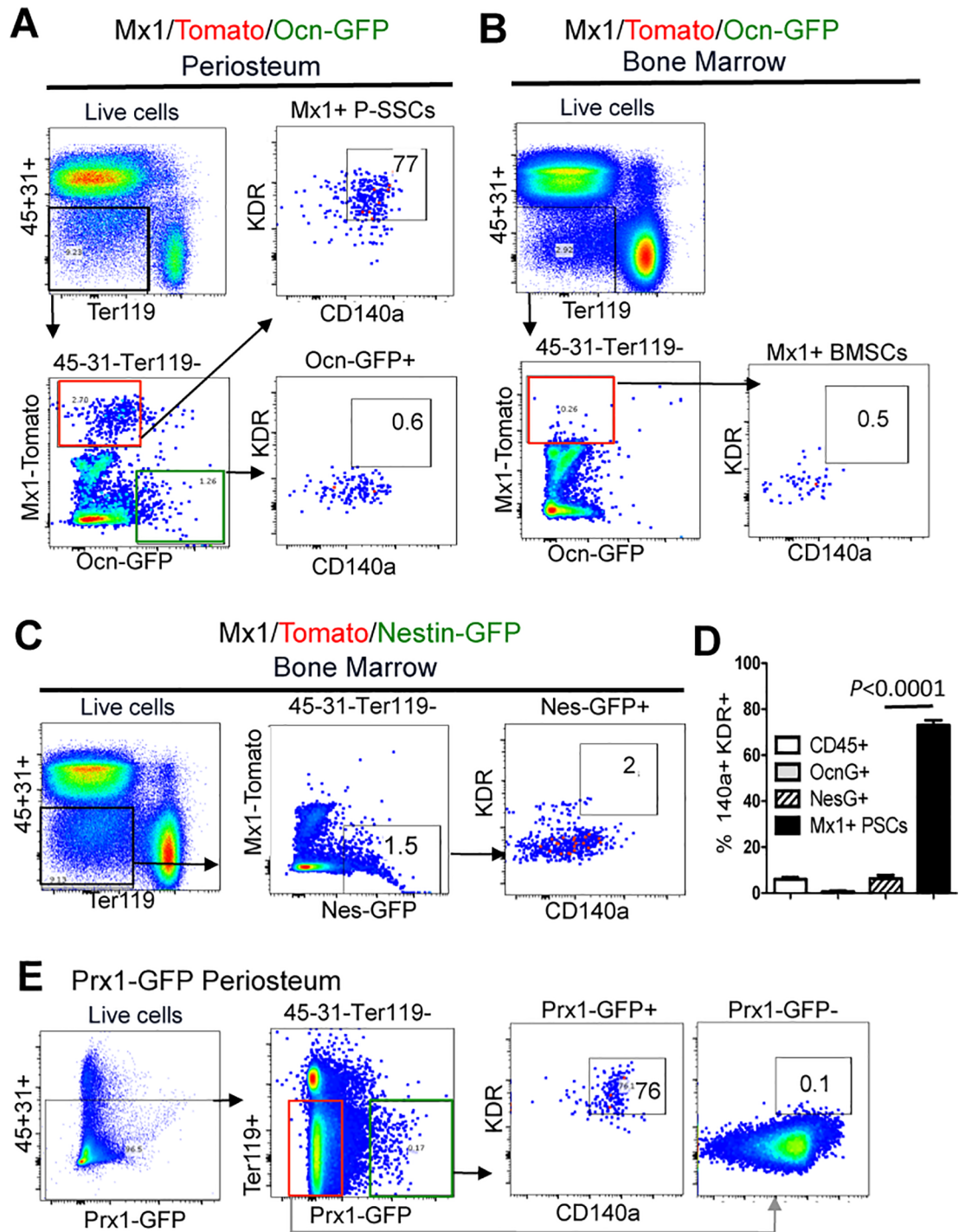


Fig 5. P-SSCs selectively express KDR. (A) Higher surface expression of KDR and CD140a in P-SSCs ($CD45^{-}CD31^{-}Ter119^{-}Mx1^{+}Ocn^{-}$) compared to periosteal osteoblast controls ($CD45^{-}CD31^{-}Ter119^{-}Mx1^{+}Ocn^{+}$) from $Mx1^{Cre}; Rosa^{Tomato}; Osteocalcin^{GFP}$ mice. (B) Undetectable expression of KDR in $Mx1^{+}$ BMSCs ($CD45^{-}CD31^{-}Ter119^{-}Mx1^{+}Ocn^{-}$) in the same mice ($Mx1^{Cre}; Rosa^{Tomato}; Osteocalcin^{GFP}$). (C) $KDR^{+}CD140a^{+}$ FACS analysis of BM-SSCs ($CD45^{-}CD31^{-}Ter119^{-}Mx1^{+}Nes^{+}$) from $Mx1^{Cre}; Rosa26^{Tomato}; Nestin^{GFP}$ transgenic mice similarly shows decreased expression of KDR in BM-SSCs. (D) Summary of FACS analysis demonstrates that $Mx1^{+}Ocn^{-}$ P-SSCs uniquely express KDR and CD140a (77%) compared to BM-SSCs and control populations ($n = 3, p < 0.0001$). (E) Confirmation of the selective expression of KDR and CD140a in $Prx1^{GFP+}$ P-SSCs.

<https://doi.org/10.1371/journal.pone.0190909.g005>

cells, we carefully isolated $Mx1^+$ SSC populations by using SSC surface markers (CD105 and CD140a) and by negatively selecting against CD45⁺ hematopoietic lineage cells and CD31⁺ endothelial lineage cells as previously described. In addition we found $Mx1^+$ cells are present in both the BM and periosteal tissue compartments, so we transiently label $Mx1^+$ cells to isolate BM-SSCs and P-SSCs from each compartment, respectively. For BM-SSCs, $Mx1^+$ cells were further purified by co-expression with $Nestin^{GFP}$. By comparison, the P-SSC population was further purified by removing Ocn^{GFP+} adult osteolineage cells from the population. Inherently, our BM-SSC population was a more highly purified population than the P-SSC population used in this study, which is important to recognize for data interpretation. Still, both of these populations were found to express *Leptin Receptor* and *Gremlin 1*, showing that these populations are comparable to previously reported SSC populations, and this also supported our microarray findings.

We additionally isolated CD51⁺ cells as another population representing BMSCs for comparison to P-SSCs [17]. This marker along with PDGFR-alpha (CD140a) had previously been shown to be expressed on $Nestin^{GFP+}$ BM-SSCs [17]. However, in our study, we found that this population was far different from the $Mx1^+Nes^{GFP+}$ BM-SSC population (Fig 2G). In comparison, $Mx1^+Nes^{GFP+}$ BM-SSCs and $Mx1^+Ocn^-$ P-SSCs were more closely related than CD51⁺ cells were than with either of these cell populations. This finding suggests that CD51⁺ cells may include BM-SSCs but represent a highly heterogeneous cell population (S2 Table).

From our analysis, we identified KDR as a uniquely expressed gene for $Mx1^+Ocn^-$ P-SSCs compared to BM-SSCs. KDR is also known as VEGF receptor 2 (VEGFR2) and exerts its actions via binding VEGF. This receptor is known to be widely expressed on CD31⁺ endothelial cells. While these cells could be a potential contaminant in our cell isolation of P-SSCs, we had eliminated CD31⁺ cells during our collection making this less likely. As a verification step, we performed pooled microarray analysis using gene commons data and also performed FACS analysis of $Prx1^{GFP+}$ periosteal progenitor cells, based on previous studies reporting undetectable labeling of bone marrow endothelial cells from $Prx1^{Cre}$ reporter mice [31,32]. Both of these analyses confirmed upregulation of KDR in endogenous P-SSCs (Fig 5E). With this in mind, the expression of KDR on $Mx1^+Ocn^-$ P-SSCs is interesting because P-SSCs are believed to rapidly react to bone injuries and it would represent an efficient control mechanism for both endothelial cells and P-SSCs to respond to the same signaling molecule. Thus, during states of injury or inflammation, both cells would become activated in part for an angiogenic process and in part to initiate bone repair process, which inherently go hand-in-hand. Of further note is that periosteal tissue is known to be highly vascularized, and angiogenesis likely proceeds from the periosteal tissue. In either case, we would hope to further explore KDR as a potential regulatory mechanism of P-SSCs.

As part of our analysis, we showed that P-SSCs represent a distinct population from Osx^+ cells. From prior studies, it was known that both Osx^+ cells and P-SSCs are involved in endochondral ossification. Considering that *Osx* deficiencies can cause arrest of endochondral ossification, it would follow that P-SSCs participate in this process by differentiating down an *Osx*⁺ pathway. Still, differences exist between these two cell populations because P-SSCs represent upstream progenitors.

In summary, we performed a microarray analysis on mouse $Mx1^+Nes^+$ BM-SSCs and $Mx1^+Ocn^-$ P-SSCs and found that these are a similar population of cells without apparent differences readily assessed by gene expression analysis. However, our scatter plot analysis did show potential differences in gene expression although it did not reach statistical significance. The inability to find differential gene expression may be related to the residual heterogeneity of the cell populations. Still, both populations were found to express Leptin Receptor and Gremlin 1, which are consistent with their findings as SSCs and also supported the microarray

analysis. We also found an interesting uniquely expressed gene in P-SSC, which was KDR. While the significance of this is yet to be determined, it represents an interesting gene because of its relationship to endothelial cells and the angiogenic response and the fact that periosteum is a highly vascularized tissue. Other studies to explore would be single cell analysis or exploring the possibility of environmental cues as the basis for the different functional roles between BM-SSCs and P-SSCs.

Supporting information

S1 Table. Differentially expressed genes comparing P-SSCs and BM-SSCs with controls. SSCs are compared with both CD45⁺ cells and *Osx*⁺ cells ($p < 0.05$). (TIF)

S2 Table. Numbers and p-value of genes comparing P-SSCs and BM-SSCs with CD51⁺ BMSCs. (TIF)

Acknowledgments

Research reported in this publication was supported by National Institute of Arthritis and Musculoskeletal and Skin Diseases of the National Institutes of Health under grant number 1K01AR061434 and by the Bone Disease Program of Texas Award to D.P and The Caroline Wiess Law Fund Award to D.P. We are grateful to B. Garrison and M. Kim for advice and technical assistance. We also thank J. Lee and former members of the Park laboratory and Lee laboratory for discussions. We thank M. E. Dickinson in the BCM Optical Imaging and Vital Microscopy Core, and J. Sederstrom in the BCM Cytometry and Cell Sorting Core.

Author Contributions

Data curation: Laura Ortinau, Kevin Lei.

Investigation: Lorenzo Deveza, Laura Ortinau, Dongsu Park.

Project administration: Dongsu Park.

Supervision: Dongsu Park.

Writing – original draft: Lorenzo Deveza, Dongsu Park.

Writing – review & editing: Dongsu Park.

References

1. O'Keefe RJ (2015) Fibrinolysis as a Target to Enhance Fracture Healing. *N Engl J Med* 373: 1776–1778. <https://doi.org/10.1056/NEJMcibr1510090> PMID: 26510027
2. Einhorn TA, Gerstenfeld LC (2015) Fracture healing: mechanisms and interventions. *Nat Rev Rheumatol* 11: 45–54. <https://doi.org/10.1038/nrrheum.2014.164> PMID: 25266456
3. Schindeler A, McDonald MM, Bokko P, Little DG (2008) Bone remodeling during fracture repair: The cellular picture. *Semin Cell Dev Biol* 19: 459–466. <https://doi.org/10.1016/j.semcdb.2008.07.004> PMID: 18692584
4. Hadjiargyrou M, O'Keefe RJ (2014) The convergence of fracture repair and stem cells: interplay of genes, aging, environmental factors and disease. *J Bone Miner Res* 29: 2307–2322. <https://doi.org/10.1002/jbmr.2373> PMID: 25264148
5. Bianco P, Robey PG (2015) Skeletal stem cells. *Development* 142: 1023–1027. <https://doi.org/10.1242/dev.102210> PMID: 25758217

6. Ozaki A, Tsunoda M, Kinoshita S, Saura R (2000) Role of fracture hematoma and periosteum during fracture healing in rats: interaction of fracture hematoma and the periosteum in the initial step of the healing process. *J Orthop Sci* 5: 64–70. PMID: [10664441](https://pubmed.ncbi.nlm.nih.gov/10664441/)
7. Ozaki A, Tsunoda M, Kinoshita S, Saura R (2000) Role of fracture hematoma and periosteum during fracture healing in rats: Interaction of fracture hematoma and the periosteum in the initial step of the healing process. 64–70 p.
8. Murao H, Yamamoto K, Matsuda S, Akiyama H (2013) Periosteal cells are a major source of soft callus in bone fracture. *J Bone Miner Metab* 31: 390–398. <https://doi.org/10.1007/s00774-013-0429-x> PMID: [23475152](https://pubmed.ncbi.nlm.nih.gov/23475152/)
9. Ransom RC, Hunter DJ, Hyman S, Singh G, Ransom SC, et al. (2016) Axin2-expressing cells execute regeneration after skeletal injury. *Sci Rep* 6: 36524. <https://doi.org/10.1038/srep36524> PMID: [27853243](https://pubmed.ncbi.nlm.nih.gov/27853243/)
10. Colnot C, Huang S, Helms J (2006) Analyzing the cellular contribution of bone marrow to fracture healing using bone marrow transplantation in mice. *Biochemical and Biophysical Research Communications* 350: 557–561. <https://doi.org/10.1016/j.bbrc.2006.09.079> PMID: [17022937](https://pubmed.ncbi.nlm.nih.gov/17022937/)
11. Colnot C (2009) Skeletal cell fate decisions within periosteum and bone marrow during bone regeneration. *J Bone Miner Res* 24: 274–282. <https://doi.org/10.1359/jbmr.081003> PMID: [18847330](https://pubmed.ncbi.nlm.nih.gov/18847330/)
12. Chan CK, Seo EY, Chen JY, Lo D, McArdle A, et al. (2015) Identification and specification of the mouse skeletal stem cell. *Cell* 160: 285–298. <https://doi.org/10.1016/j.cell.2014.12.002> PMID: [25594184](https://pubmed.ncbi.nlm.nih.gov/25594184/)
13. Mendez-Ferrer S, Michurina TV, Ferraro F, Mazloom AR, MacArthur BD, et al. (2010) Mesenchymal and haematopoietic stem cells form a unique bone marrow niche. *Nature* 466: 829–834. <https://doi.org/10.1038/nature09262> PMID: [20703299](https://pubmed.ncbi.nlm.nih.gov/20703299/)
14. Zhou BO, Yue R, Murphy MM, Peyer JG, Morrison SJ (2014) Leptin-receptor-expressing mesenchymal stromal cells represent the main source of bone formed by adult bone marrow. *Cell Stem Cell* 15: 154–168. <https://doi.org/10.1016/j.stem.2014.06.008> PMID: [24953181](https://pubmed.ncbi.nlm.nih.gov/24953181/)
15. Worthley DL, Churchill M, Compton JT, Tailor Y, Rao M, et al. (2015) Gremlin 1 identifies a skeletal stem cell with bone, cartilage, and reticular stromal potential. *Cell* 160: 269–284. <https://doi.org/10.1016/j.cell.2014.11.042> PMID: [25594183](https://pubmed.ncbi.nlm.nih.gov/25594183/)
16. Park D, Spencer JA, Koh BI, Kobayashi T, Fujisaki J, et al. (2012) Endogenous bone marrow MSCs are dynamic, fate-restricted participants in bone maintenance and regeneration. *Cell Stem Cell* 10: 259–272. <https://doi.org/10.1016/j.stem.2012.02.003> PMID: [22385654](https://pubmed.ncbi.nlm.nih.gov/22385654/)
17. Pinho S, Lacombe J, Hanoun M, Mizoguchi T, Bruns I, et al. (2013) PDGFR α and CD51 mark human Nestin(+) sphere-forming mesenchymal stem cells capable of hematopoietic progenitor cell expansion. *The Journal of Experimental Medicine* 210: 1351–1367. <https://doi.org/10.1084/jem.20122252> PMID: [23776077](https://pubmed.ncbi.nlm.nih.gov/23776077/)
18. Kuhn R, Schwenk F, Aguet M, Rajewsky K (1995) Inducible gene targeting in mice. *Science* 269: 1427–1429. PMID: [7660125](https://pubmed.ncbi.nlm.nih.gov/7660125/)
19. Srinivas S, Watanabe T, Lin CS, William CM, Tanabe Y, et al. (2001) Cre reporter strains produced by targeted insertion of EYFP and ECFP into the ROSA26 locus. *BMC Dev Biol* 1: 4. <https://doi.org/10.1186/1471-213X-1-4> PMID: [11299042](https://pubmed.ncbi.nlm.nih.gov/11299042/)
20. Vrsnjic D, Kalajzic I, Gronowicz G, Aguila HL, Clark SH, et al. (2001) Conditional ablation of the osteoblast lineage in Col2.3deltatg transgenic mice. *J Bone Miner Res* 16: 2222–2231. <https://doi.org/10.1359/jbmr.2001.16.12.2222> PMID: [11760835](https://pubmed.ncbi.nlm.nih.gov/11760835/)
21. Park D, Spencer JA, Lin CP, Scadden DT (2014) Sequential in vivo imaging of osteogenic stem/progenitor cells during fracture repair. *J Vis Exp* 87: e51289.
22. Mignone JL, Kukekov V, Chiang AS, Steindler D, Enikolopov G (2004) Neural stem and progenitor cells in nestin-GFP transgenic mice. *J Comp Neurol* 469: 311–324. <https://doi.org/10.1002/cne.10964> PMID: [14730584](https://pubmed.ncbi.nlm.nih.gov/14730584/)
23. Rodda SJ, McMahon AP (2006) Distinct roles for Hedgehog and canonical Wnt signaling in specification, differentiation and maintenance of osteoblast progenitors. *Development* 133: 3231–3244. <https://doi.org/10.1242/dev.02480> PMID: [16854976](https://pubmed.ncbi.nlm.nih.gov/16854976/)
24. Pinho S, Lacombe J, Hanoun M, Mizoguchi T, Bruns I, et al. (2013) PDGFR α and CD51 mark human nestin+ sphere-forming mesenchymal stem cells capable of hematopoietic progenitor cell expansion. *J Exp Med* 210: 1351–1367. <https://doi.org/10.1084/jem.20122252> PMID: [23776077](https://pubmed.ncbi.nlm.nih.gov/23776077/)
25. Mendez-Ferrer S, Michurina TV, Ferraro F, Mazloom AR, MacArthur BD, et al. (2010) Mesenchymal and haematopoietic stem cells form a unique bone marrow niche. *Nature* 466: 829–834. <https://doi.org/10.1038/nature09262> PMID: [20703299](https://pubmed.ncbi.nlm.nih.gov/20703299/)

26. Sacchetti B, Funari A, Michienzi S, Di Cesare S, Piersanti S, et al. (2007) Self-renewing osteoprogenitors in bone marrow sinusoids can organize a hematopoietic microenvironment. *Cell* 131: 324–336. <https://doi.org/10.1016/j.cell.2007.08.025> PMID: 17956733
27. Mizoguchi T, Pinho S, Ahmed J, Kunisaki Y, Hanoun M, et al. (2014) Osterix marks distinct waves of primitive and definitive stromal progenitors during bone marrow development. *Dev Cell* 29: 340–349. <https://doi.org/10.1016/j.devcel.2014.03.013> PMID: 24823377
28. Ema M, Takahashi S, Rossant J (2006) Deletion of the selection cassette, but not cis-acting elements, in targeted Flk1-lacZ allele reveals Flk1 expression in multipotent mesodermal progenitors. *Blood* 107: 111–117. <https://doi.org/10.1182/blood-2005-05-1970> PMID: 16166582
29. Seita J, Sahoo D, Rossi DJ, Bhattacharya D, Serwold T, et al. (2012) Gene Expression Commons: an open platform for absolute gene expression profiling. *PLoS One* 7: e40321. <https://doi.org/10.1371/journal.pone.0040321> PMID: 22815738
30. Worthley Daniel L, Churchill M, Compton Jocelyn T, Taylor Y, Rao M, et al. Gremlin 1 Identifies a Skeletal Stem Cell with Bone, Cartilage, and Reticular Stromal Potential. *Cell* 160: 269–284. <https://doi.org/10.1016/j.cell.2014.11.042> PMID: 25594183
31. Ouyang Z, Chen Z, Ishikawa M, Yue X, Kawanami A, et al. (2013) Prx1 and 3.2kb Col1a1 promoters target distinct bone cell populations in transgenic mice. *Bone* 58: 136–145.
32. Greenbaum A, Hsu YM, Day RB, Schuettpelz LG, Christopher MJ, et al. (2013) CXCL12 in early mesenchymal progenitors is required for haematopoietic stem-cell maintenance. *Nature* 495: 227–230. <https://doi.org/10.1038/nature11926> PMID: 23434756